Chapter 27
Investigation of MRR in Wire-Cut Electrical Discharge Machining of Incoloy-800 Using Statistical Approach

Sudhir Ranjan and Ravi Pratap Singh

Abstract Superalloys comprise one of the bright categories of alloys that possess excellent mechanical strength at elevated temperatures, superior surface stability, magnificent creep resistance, and corrosion and oxidation resistance. The present article has been attempted to investigate the effect of several input machining variables on the material removal rate in wire-cut electrical discharge machining of Incoloy-800 superalloy. Pulse on time, pulse off time, and peak current have been selected as machining parameters for the study. According to the Taguchi method based on robust design, a L9 orthogonal array is employed for the experimentation. The analysis of variance test and the optimization of the selected machining response have also been performed to reveal out the impact and the behavior of the considered input factors on the machining responses statistically. The peak current factor has been revealed as the most dominating parameter for the MRR followed by pulse on time and pulse off time. The optimized parametric setting for the studied machining response (MRR) has been observed as: pulse on time −2 μs, pulse off time −4 μs, and peak current −3 A, i.e., A2B1C3. At the optimized setting, the confirmatory experiment value for MRR has been revealed as 1.5439 mm/min, which is improved by 2.57% than the previously attained best value of MRR.

Keywords Wire-EDM · Incoloy-800 · Super alloy · MRR · Taguchi approach

Nomenclature

T_{on}	Pulse on time
T_{off}	Pulse off time
I_p	Peak current
WEDM	Wire electrical discharge machining

S. Ranjan · R. P. Singh (✉)
Department of Industrial and Production Engineering, Dr. B. R. Ambedkar National Institute of Technology, Jalandhar 144011, Punjab, India
e-mail: singhrp@nitj.ac.in

M. Tyagi et al. (eds.), *Optimization Methods in Engineering*,
Lecture Notes on Multidisciplinary Industrial Engineering,
https://doi.org/10.1007/978-981-15-4550-4_27

MRR Material removal rate

27.1 Introduction

Superalloys comprise one of the bright categories of alloys that possess excellent mechanical strength at elevated temperatures, superior surface stability, magnificent creep resistance, and corrosion and oxidation resistance. They have a FCC structure of austenitic type with a base of nickel, iron, cobalt, or a blend of them. They have a very high strength-to-weight ratio, are resistant to erosion, and possess metallurgic stability at elevated temperatures. Through solid solution strengthening, superalloys develop high temperature strength. The main contribution in the field of superalloys is contributed by aerospace and power industries along with the chemical industries. As they are resistant to corrosion and oxidation, therefore they have a great advantage to be used in the chemical industries. Elements like aluminum and chromium provide corrosion and oxidation resistance to superalloys as these alloys are intended to use for elevated temperature applications and this property of resistance is of great importance. They are also used in other high temperature applications like nuclear reactors and gas turbines other than their applications in aerospace industry.

Incoloy-800 is an iron base superalloy having main composition of iron–nickel–chromium. It possesses sufficient resistance to oxidation and carburization at elevated temperatures. It is of high use in petrochemical industry as it does not form embrittling sigma phase after long time exposure at 1200 °F. It is also highly resistant to stress corrosion cracking. On the other hand, in spite of its superior qualities its effective machining is still a challenge with the traditional machining methods. Incoloy-800 welds to the cutting tool if machined by these traditional methods because of its chemically reactive nature, leading to the premature tool failure. So for its productive machining, non-traditional machining methods are preferred.

In the present scenario of non-traditional machining methods, wire electrical discharge machining (WEDM) is one of the fastest extensive growing processes. Wire EDM can produce complex shapes with better surface finish and high level of accuracy and precision. Micro-machining operations and machining operations can be performed on it. It is continuously increasing popularity in aerospace, manufacturing, automobile, medicine, injection molding, and other various industries making it a hot topic of research.

Mathew [1] investigated the parameters for machining a difficult-to-machine superalloy: Inconel X-750 and Waspaloy. They analyzed the tool wear, turning forces, and surface roughness in dry turning of these superalloys. The higher amount of force is obtained for Waspaloy than Inconel X-750 for all the cutting conditions because of its higher tensile strength. Welling [2] studied the surface integrity differences between broaching and grinding compared to wire EDM on the Inconel 718 superalloy. The three-cut strategy is specially developed for the brass wire electrodes. For broaching, separate specimen with 3.2 mm thickness is selected. Xavior et al. [3]

machined Inconel 718 on wire EDM and studied the effect of recast layer thickness on its mechanical characteristics. The parameters chosen are current pulse duration, peak discharge current, pulse off time, and gap voltage as it was studied that these parameters influence the recast layer thickness. Mandal et al. [4] examined the interrelationships between process parameters and performance measures of Nimonic C-263 superalloy machined on wire EDM. The process parameters chosen are pulse off time, rate flow of dielectric, servo voltage, and pulse on time. Mandal et al. [5] analyzed the wire EDM input parameters on Kerf width and surface integrity for Al 6061 alloy and found that the major factor affecting surface roughness was pulse on time followed by pulse off time and wire tension. The reasoning and explanations for surface roughness behavior have also been elaborated in several advanced machining-based studies [6–8]. Rajyalakshmi et al. [9] machined Inconel 825 on wire EDM and optimized its various process parameters by using Taguchi gray relation analysis. The process parameters taken are pulse off time, corner servo voltage, pulse on time, flushing pressure, servo feed rate, wire tension, wire feed, spark gap voltage. Using the gray grade value, ANOVA is formulated for identifying the significant factors. Rao et al. [10] machined Inconel 690 and applied modified flower pollination algorithm (FPA) to optimize parameters of wire EDM. The responses are compared with RSM. Goyal et al. [11] used wire EDM to optimize the surface roughness of Inconel 625. For design of experiments, Taguchi L_{18} ($2^1 \times 3^5$) orthogonal array is used. Plain and cryogenic treated these two different diffused wire tool electrodes were used. Tanjilul et al. [12] studied debris removal in EDM drilling of Inconel 718 and examined the EDM flushing mechanism and debris size for efficient debris removal. Furthermore, several studies have been attempted in the domain of optimization and modeling of process variables [13–16]. Nain et al. [17] examined the effects of various input parameter responses—surface roughness and effects of recast layer using fuzzy and BP-ANN model. Rao et al. [18] optimized wire EDM process while machining Inconel 690 by applying modified (CSA) cuckoo search algorithm.

In view of above discussions, the present experimental study has been attempted to investigate the effect of several input machining variables on the considered performance characteristic in wire-cut electrical discharge machining of Incoloy-800 superalloy. The analysis of variance test and the optimization of the selected machining response have also been performed to reveal out the impact and the behavior of the considered input factors on the machining responses statistically. Table 27.1 shows the literature review.

27.2 Materials and Methods

The experimental work has been carried out on wire EDM (ELECTRONICA ELEKTRA MAXICUT 734) as shown in Fig. 27.1. In this study, Incoloy-800 superalloy plate of 200 × 150 mm^2 area and 12 mm thickness has been used as the workpiece whose composition, properties, and workpiece figure are shown in Tables 27.2, 27.3

Table 27.1 Literature review

S. no.	Investigators	Work material	Process used	Process parameters	Response studied	Research findings
1	Spedding et al. [19]	AISI 420	Wire EDM	Wire mechanical tension, pulse width, the time between two pulses, and wire speed	Surface texture and cutting speed	Cutting speed and surface texture are determined by time between two pulses and pulse width. Greater the spark discharge power, greater is the diameter of the crater and MRR. Both RSM and ANN fit the process successfully, but the ANN achieves a closer fit and has higher predictive capability to surface texture and cutting speed
2	Dauw et al. [20]	Theoretical study	Wire EDM	Theoretical study	Average cutting speed, machining cost, surface finish, discharge current, machine design	Average cutting speed has increased, relative machining cost has reduced, surface finish and machine tolerances have been improved, discharge current produced by machine has increased, and machine design concept has been improved

(continued)

Table 27.1 (continued)

S. no.	Investigators	Work material	Process used	Process parameters	Response studied	Research findings
3	Yan et al. [21]	Boron-doped polycrystalline composite diamond (BD-PCD)	Wire EDM	Peak current, discharge duration, pulse off time, and pulse on time	Surface finish, surface quality, surface damages	Iso pulse generator provides more evenly distributed discharge energy to the spark gap than the Iso frequency pulse generator. Iso pulse generator also achieved less damaged layer and high surface quality
4	Daniel et al. [22]	Molybdenum wire of 0.25 mm diameter	Wire EDM	Flushing pressure, pulse off time, pulse on time, servo voltage, wire tension, and wire feed rate	Material removal rate	ANN model can successfully be applied in wire EDM process to predict the machining responses. The model developed gives close results to experimental values. The obtained optimum parameters are T_{on} of 114, T_{off} of 40, F_p of 10, WT of 750, S_v of 15, and WF of 8

(continued)

Table 27.1 (continued)

S. no.	Investigators	Work material	Process used	Process parameters	Response studied	Research findings
5	Mandal et al. [5]	Al 6061 alloy	Wire EDM	Servo voltage, pulse off time, pulse on time, and wire tension	Surface roughness and Kerf width	T_{on} and S_V are most significant parameters affecting Kerf width with a percentage of 69.41 and 19.51%, respectively, for a confidence level of 95% T_{on}, T_{off}, and WT are most significant parameters affecting surface roughness with a contribution of 67.10, 19.01, and 12.31, respectively
6	Pramanik et al. [23]	Al 6061 t6 alloy	Wire EDM	Wire feed rate, pulse off time, pulse on time, and gap voltage	MRR and surface roughness	For MRR, pulse off time is the most important factor followed by wire feed rate, gap voltage, and pulse on time having a percentage contribution of 74.52, 11.02, 13.08, and 1.36%, respectively For SR, pulse on time is the most dominating factor having a percentage contribution of 59.30%

(continued)

Table 27.1 (continued)

S. no.	Investigators	Work material	Process used	Process parameters	Response studied	Research findings
7	Magabe et al. [24]	$Ni_{55.8}Ti$ shape memory alloy	Wire EDM	Spark gap voltage, wire feed, pulse off time, pulse on time	Surface roughness and MRR	At higher voltage, pulse on time, and wire feed rate, an increment in material removal rate is observed
8	Huang et al. [25]	SKD11 alloy steel	Wire EDM	Fluid pressure, wire velocity, pulse off time, wire tension, pulse on time, and table feed rate	Surface roughness and MRR	Larger values of pulse on time, table feed rate, and pulse off time are better for a better MRR, while small values of wire velocity and wire tension are better. Medium values of fluid pressure are also better for a high MRR Surface roughness and gap width are mainly affected by pulse on time

(continued)

Table 27.1 (continued)

S. no.	Investigators	Work material	Process used	Process parameters	Response studied	Research findings
9	Sahoo et al. [26]	High carbon, high chromium steel	Wire EDM	Wire feed rate, pulse width time, and pulse off time	Surface roughness, MRR, and Kerf width	With increase in pulse on time, the MRR increases rapidly and slowly with increase in wire feed rate. With increase in pulse off time, it decreases at a slower rate Kerf width increases rapidly with increase in pulse duration time and slowly with increase in wire feed rate. It also decreases at a slower rate with increase in pulse off time

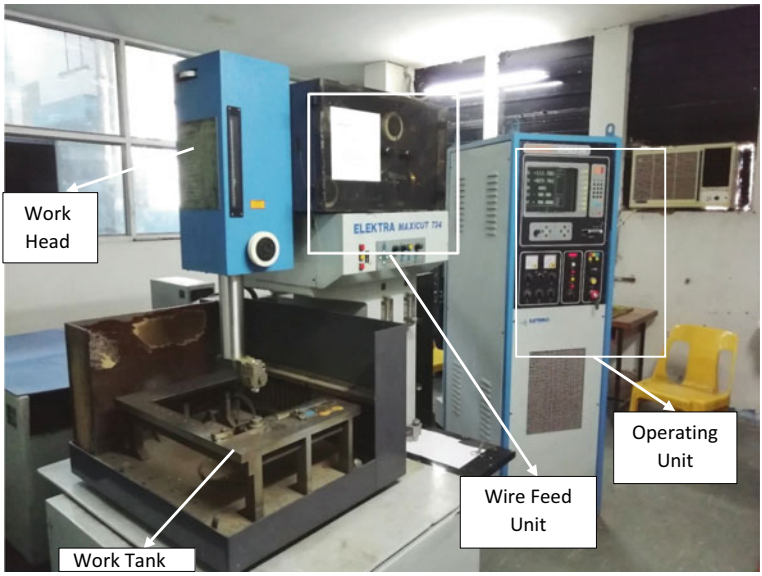

Fig. 27.1 Wire EDM machine setup for the experimentation

Table 27.2 Composition of Incoloy-800

Element	Fee	Cr	Ni	Cu	Al	C	S	Ti
Content (%)	39.5 min	19–23	30–35	0.5 max	0.15–0.60	0.10 max	0.015 max	0.15–0.60

Table 27.3 Properties of Incoloy-800

Property	Metric	Imperial
Density	7.94 gm/cm^3	0.287 lb/in^3
Tensile strength	600 MPa	87 ksi
Yield strength	275 MPa	39.9 ksi
Elongation at break	45%	45%
Melting temperature range	1357–1385 °C	2475–2525 °F

and Fig. 27.2, respectively. Soft brass wire of 0.25 mm diameter has been used as the tool electrode. Deionized water has been used as dielectric fluid which is flushed continuously through the gap along the wire and the sparking area to remove the debris produced during erosion. Figure 27.3 shows the dielectric flushing unit. The machine is programmed by using a NC code. Square cuts of 8 mm side have been fabricated from the workpiece as shown in Fig. 27.4.

Design of experiments has been widely employed in the previous research articles by considering several working factors and responses [27–31]. According to the Taguchi method based on robust design, a L9 orthogonal array is employed for the

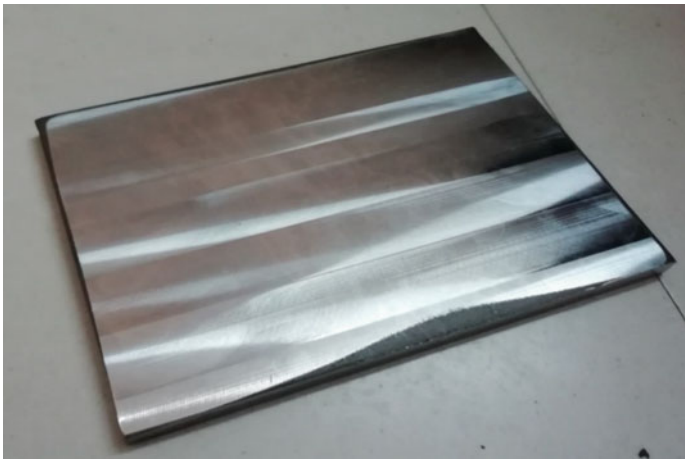

Fig. 27.2 Incoloy-800 workpiece for the experimentation

Fig. 27.3 Dielectric flushing unit

experimentation. Based on pilot experiments carried, pulse on time, pulse off time, and peak current have been selected as the input process parameters and their levels are mentioned in Table 27.4. The various machining inputs have been kept constant as: servo voltage at 60 V, wire feed rate at 6 m/min, and the wire tension at 700 N.

27.3 Results and Discussion

The experiments have been conducted as per the Taguchi L9 orthogonal array. The experiments have been replicated twice to distribute the error uniformly. The design matrix along with the studied response values has been detailed in Table 27.5.

Fig. 27.4 Machined workpiece sample

Table 27.4 Controllable process parameters and their levels

Factor	Parameter	Symbol	Level 1	Level 2	Level 3
1	Pulse on time	T_{on} (μs)	1	2	3
2	Pulse off time	T_{off} (μs)	4	5	6
3	Peak current	I_p (A)	1	2	3

Table 27.5 Design matrix and the response values (MRR)

Run	T_{on}	T_{off}	I_p	MRR (mean value)
1	1	4	1	0.7048
2	1	5	2	0.7128
3	1	6	3	1.2811
4	2	4	2	0.8064
5	2	5	3	1.4856
6	2	6	1	0.7218
7	3	4	3	1.5142
8	3	5	1	0.7438
9	3	6	2	0.7214

Table 27.6 Analysis of variance (ANOVA) for S/N ratio

Source	DF	Seq SS	Adj SS	Adj MS	F	P	
T_{on}	2	1.2195	1.2195	0.6097	100.86	0.010	Significant
T_{off}	2	0.8432	0.8432	0.4216	69.74	0.014	Significant
I_P	2	66.1612	66.1612	33.0806	5471.83	0.000	Significant
Residual error	2	0.0121	0.0121	0.0060			
Total	8	68.2360					

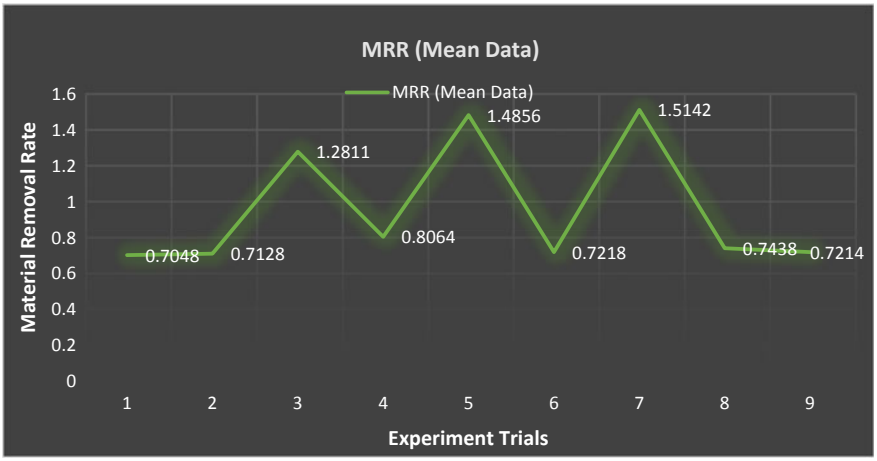

Fig. 27.5 Variation of material removal rate under several trial runs

After attaining the MRR values, the analysis of variance test has been performed as shown in Table 27.6 and Fig. 27.5. shows variation of material removal rate under several trial runs. From the ANOVA results of MRR, it can be observed that T_{on}, T_{off}, and I_p are influencing the MRR. As the T_{on} increases, the MRR also gets increased with it but after attaining a highest value it slightly decreases with further increase in T_{on}. When the pulse on time was 1 μs, the MRR has been recorded minimum and highest at 2 μs with the very slight decrease at 3 μs. MRR gets decreased with the increase in T_{off} continuously at all levels. With the increase in I_p from 1 to 2 A, the MRR somewhat gets increased but it shows a drastic increase when I_p increases from 2 to 3 A. Figure 27.6 shows the main effects plot for MRR (S/N) mean data.

The peak current factor has been revealed as the most dominating parameter for the MRR followed by pulse on time, pulse off time, and wire feed rate. The optimized parametric setting for the studied machining response (MRR) has been observed as: pulse on time −2 μs, pulse off time −4 μs, and peak current −3 A, i.e., A2B1C3. At the optimized setting, the confirmatory experiment value for MRR has been revealed as 1.5439 mm/min, which is improved by 2.57% than the previously attained best value of MRR.

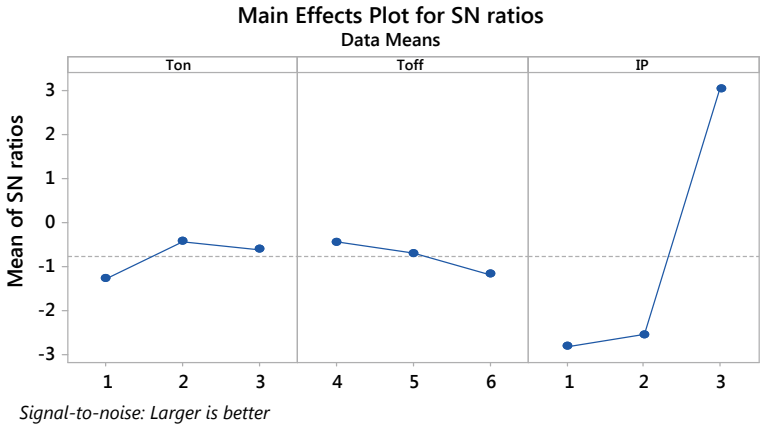

Fig. 27.6 Main effects plot for MRR (S/N)

27.4 Conclusion

The following conclusions can be drawn from the present experimental study. These are as below:

1. Peak current and pulse on time have been recorded as the most influencing parameters for the MRR. An extreme increase in MRR has been observed when the peak current is increased from 2 to 3 A. It also shows an increase with the increase in pulse on time (from 1 to 2 A), but it slightly gets decreased with further increase in the pulse on time (from 2 to 3 A).
2. The optimized parametric setting for the studied machining response (MRR) has been observed as A2B1C3 (pulse on time −2 μs, pulse off time −4 μs, and peak current −3 A).
3. At the optimized setting, the confirmatory experiment value for MRR has been revealed as 1.5439 mm/min, which is improved by 2.57% than the previously attained best value of MRR.

References

1. Mathew, A.T.: Innovative Design, Analysis and Development Practices in Aerospace and Automotive Engineering (I-DAD 2018) (2019)
2. Welling, D.: Results of surface integrity and fatigue study of wire-EDM compared to broaching and grinding for demanding jet engine components made of Inconel 718. Procedia CIRP **13**, 339–344 (2014)
3. Xavior, M.A., Ashwath, P., Ali, H., Moideen, A., Banu, P., Illanthendral, Sancylal, S.: Effect of recast layer thickness on the mechanical characteristics of INCONEL 718 machined by spark EDM process. Mater. Today: Proc. **5**(2), 8249–8255 (2018)

4. Mandal, A., Dixit, A.R., Das, A.K., Mandal, N.: Modeling and optimization of machining nimonic C-263 superalloy using multicut strategy in WEDM. Mater. Manuf. Process. **31**(7), 860–868 (2016)
5. Mandal, K., Sarkar, S., Mitra, S., Bose, D.: Innovation in Materials Science and Engineering (2019)
6. Singh, R.P., Singhal, S.: Rotary ultrasonic machining: a review. Mater. Manuf. Process. **31**, 1795–1824 (2016)
7. Singh, R.P., Singhal, S.: Investigation of machining characteristics in rotary ultrasonic machining of alumina ceramic. Mater. Manuf. Process. **32**, 309–326 (2017)
8. Singh, R.P., Tyagi, M., Kataria, R.: Selection of the optimum hole quality conditions in manufacturing environment using MCDM approach: a case study. Operations Management and Systems Engineering, pp. 133–152. Springer, Singapore (2019)
9. Rajyalakshmi, G., Venkata Ramaiah, P.: Multiple process parameter optimization of wire electrical discharge machining on Inconel 825 using Taguchi grey relational analysis. International Journal of Advanced Manufacturing Technology, 69(5–8), 1249–1262 (2013)
10. Sreenivasa Rao, M., Venkata Naresh Babu, A., Venkaiah, N.: Modified flower pollination algorithm to optimize WEDM parameters while machining Inconel-690 alloy. Mater. Today: Proc. **5**(2), 7864–7872 (2018)
11. Goyal, A., Pandey, A., Sharma, P.: Investigation of surface roughness for Inconel 625 using wire electric discharge machining. IOP Conf. Ser. Mater. Scie. Eng. **377**(1) (2018)
12. Tanjilul, M., Ahmed, A., Kumar, A.S., Rahman, M.: A study on EDM debris particle size and flushing mechanism for efficient debris removal in EDM-drilling of Inconel 718. J. Mater. Process. Technol. **255**, 263–274 (2018)
13. Singh, R.P., Singhal, S.: Rotary ultrasonic machining of macor ceramic: an experimental investigation and microstructure analysis. Mater. Manuf. Process. **32**, 927–939 (2017)
14. Singh, R.P., Singhal, S.: Experimental investigation of machining characteristics in rotary ultrasonic machining of quartz ceramic. J. Mater. Des. Appl. **232**, 870–889 (2018)
15. Singh, R.P., Kataria, R., Kumar, J., Verma, J.: Multi-response optimization of machining characteristics in ultrasonic machining of WC-Co composite through Taguchi method and grey-fuzzy logic. AIMS Mater. Sci. **5**, 75–92 (2018)
16. Singh, R.P., Kumar, J., Kataria, R., Singhal, S.: Investigation of the machinability of commercially pure titanium in ultrasonic machining using graph theory and matrix method. J. Eng. Res. **3**, 75–94 (2015)
17. Nain, S.S., Sihag, P., Luthra, S.: Performance evaluation of fuzzy-logic and BP-ANN methods for WEDM of aeronautics super alloy. MethodsX **5**, 890–908 (2018)
18. Sreenivasa Rao, M., Venkaiah, N.: A modified cuckoo search algorithm to optimize wire-EDM process while machining Inconel-690. J. Braz. Soc. Mech. Sci. Eng. **39**(5), 1647–1661 (2017)
19. Spedding, T.A., Wang, Z.Q.: Study on modeling of wire EDM process. J. Mater. Process. Technol. **69**, 18–28 (1997)
20. Dauw, D.F., Albert, L.: About the evolution of wire tool performance in wire EDM. CIRP Ann. Manuf. Technol. **41**, 221–225 (1992)
21. Yan, M.T., Cheng, Y.C., Luo, S.Y.: Improvement of wire electrical discharge machining characteristics in machining boron-doped polycrystalline diamond using a novel Iso-pulse generator. Int. J. Precis. Eng. Manuf. **20**, 159–166 (2019)
22. Daniel, G.: Optimization of material removal rate in wire-EDM using genetic algorithms. Int. J. Appl. Eng. Res. **14**, 313–315 (2019)
23. Pramanik, D., Kuar, A.S., Bose, D.: Renewable Energy and its Innovative Technologies. Springer, Singapore (2018)
24. Magabe, R., Sharma, N., Gupta, K., Paulo Davim, J.: Modeling and optimization of wire-EDM parameters for machining of $Ni_{55.8}Ti$ shape memory alloy using hybrid approach of Taguchi and NSGA-II. Int. J. Adv. Manuf. Technol. (2019). https://doi.org/10.1007/s00170-019-03287-z
25. Huang, J.T., Liao, Y.S.: Optimization of machining parameters of wire-EDM based on grey relational and statistical analyses. Int. J. Prod. Res. **41**, 1707–1720 (2003)

26. Sahoo, S.K., Naik, S.S., Rana, J.: Micro and Nano Machining of Engineering Materials. Springer, Singapore (2019)
27. Singh, R., Singh, R.P., Tyagi, M., Kataria, R.: Investigation of dimensional deviation in wire EDM of M42 HSS using cryogenically treated brass wire. Mater. Today: Proc. (2019). https://doi.org/10.1016/j.matpr.2019.08.028
28. Singh, R.P., Singhal, S.: An experimental study on rotary ultrasonic machining of macor ceramic. J. Engg. Manuf. **232**, 1221–1234 (2018)
29. Singh, R.P., Singhal, S.: Rotary ultrasonic machining of alumina ceramic: experimental study and optimization of machining responses. J. Eng. Res. **6**, 01–24 (2018)
30. Tyagi, M., Panchal, D., Singh, R.P., Sachdeva, A.: Modeling and analysis of critical success factors for implementing the IT-based supply-chain performance system. Operations Management and Systems Engineering, pp. 51–67. Springer, Singapore (2019)
31. Singh, R.P., Kataria, R., Singhal, S.: Decision-making in real-life industrial environment through graph theory approach. In: Computer Architecture in Industrial, Biomechanical and Biomedical Engineering. IntechOpen (2019). https://doi.org/10.5772/intechopen.82011